ENVIRONMENTAL RESEARCH
LETTERS

LETTER • **OPEN ACCESS**

Unveiling the pivotal influence of sea spray heat fluxes on hurricane rapid intensification

To cite this article: Sinil Yang *et al* 2024 *Environ. Res. Lett.* **19** 114058

ENVIRONMENTAL RESEARCH
LETTERS

OPEN ACCESS

RECEIVED
11 June 2024

REVISED
4 September 2024

ACCEPTED FOR PUBLICATION
24 September 2024

PUBLISHED
14 October 2024

LETTER

Unveiling the pivotal influence of sea spray heat fluxes on hurricane rapid intensification

Sinil Yang[1], DW Shin[2], Steven Cocke[2], Chaehyeon Chelsea Nam[3], Mark Bourassa[2,3], Dong-Hyun Cha[4] and Baek-Min Kim[5,*]

[1] APEC Climate Center, Busan 48058, Republic of Korea
[2] Center for Ocean-Atmospheric Prediction Studies, Florida State University, Tallahassee, FL 32306, United States of America
[3] Department of Earth, Ocean and Atmospheric Science, Florida State University, Tallahassee, FL 32306, United States of America
[4] Department of Civil, Urban, Earth and Environmental Engineering, Ulsan National Institute of Science and Technology, Ulsan 44919, Republic of Korea
[5] Division of Earth Environmental System Science Major of Environmental Atmospheric Sciences, Pukyong National University, Busan 48513, Republic of Korea
* Author to whom any correspondence should be addressed.

E-mail: baekmin@pknu.ac.kr

Keywords: hurricanes, sea spray, spray-mediated heat fluxes, rapid intensification, hurricane–ocean interaction

Supplementary material for this article is available online

Abstract

Predicting rapid hurricane intensification remains a challenge, partially due to neglected factors like sea spray-mediated heat flux. To shed light on the specific roles of spray-mediated sensible and latent heat fluxes, we conducted sensitivity experiments with heat flux parameterizations. Our results demonstrate that the inclusion and variation of the spray-mediated sensible heat significantly reduce model errors when compared against dropsonde data. These findings uniquely quantify the pivotal role of spray-mediated sensible heat flux in accurately predicting hurricane rapid intensification compared to previous studies. Without sea spray processes, ocean-coupled model simulations could not reproduce the steep intensification rate observed in multi-case studies of four high-impact hurricanes. This study also highlights that dropsonde data, as well as directly observed flux, is useful in minimizing uncertainty in the flux parameterization used for hurricane simulations. In this paper, we show how spray-mediated heat flux affects hurricane energetics through turbulent heat exchange and subsequent humid air inflow through primary and secondary circulations. Our findings provide new insights into the transformative role of sea spray in turbulent heat exchange that drives rapid hurricane intensification.

1. Introduction

Despite several decades of rigorous research to enhance hurricane intensity predictions, state-of-the-art numerical models continue to fall short in reproducing observed hurricane intensity (Black *et al* 2007, Rogers *et al* 2013, Emanuel *et al* 2023). This ongoing challenge highlights a crucial gap in our understanding of air–sea interactions during hurricane intensification. Since the late 20th century, the incorporation of sea spray-mediated heat fluxes into existing interfacial heat fluxes has emerged as a promising avenue (Andreas 1992, Fairall *et al* 1994, Andreas and Decosmo 2002). Large amounts of sea spray are generated by breaking ocean waves under strong winds in hurricanes, and spray-mediated sensible heat and water vapor within the shallow interfacial layer above the sea surface fundamentally influence hurricane intensity. As highlighted by Andreas and Emanuel (2001), the inclusion of sea spray in numerical models can significantly increase air–sea heat and moisture exchanges. However, this promising potential remains underutilized in hurricane research.

Advancements in formulating spray-mediated heat fluxes have been driven by laboratory and idealized studies (Andreas and Emanuel 2001, Fairall *et al* 2009, Bao *et al* 2011, Bianco *et al* 2011, Liu *et al* 2011, Staniec *et al* 2021, Sroka and Emanuel 2022). Among these studies, the sequential development by Andreas provides a fundamental framework for developing

sea spray flux parameterization in numerical models (Andreas 2003, Andreas *et al* 2008, 2015). The Andreas scheme includes two key parameters, α and β, which control the magnitude of spray-mediated latent and sensible heat fluxes (Andreas *et al* 2015) (hereafter AN15). β varies widely across studies, relative to α, mainly due to the limited availability of observations, ranging from 5.7 (Andreas 2003) to 15.15 (AN15). An increase in β results in a corresponding increase in spray-mediated sensible heat flux. However, in the literature, we still do not have a strong consensus on the proper choice of α and β in hurricane simulations.

Several recent studies explored the sea spray effect on hurricane intensification by applying the parameterization described in AN15. All these case studies exhibited some positive impacts on hurricane prediction (Lan *et al* 2022, Xu *et al* 2022, 2023). Essentially, the generation of sea spray depends on the detailed status of wave height and whitecap fraction, which can be provided by a wave model. Instead of using a wave-coupled model, most previous studies rely on the simplistic assumption of wave property variables, which merely depend on the 10 m wind speed provided by the atmospheric model (Andreas and Monahan 2000). However, such simplifications are notably inaccurate for high winds exceeding 20 m s^{-1} (Holthuijsen *et al* 2012).

Our study employs the Coupled-Ocean–Atmosphere–Wave–Sediment Transport (COAWST) modeling framework (Warner *et al* 2010) and modifies a bulk flux parameterization, as described in AN15, to be suitable for the wave-coupled model. To investigate the impact of sea spray, we examine four major Atlantic hurricanes: Ida (2021), Harvey (2017), Michael (2018), and Ian (2022), which caused significant economic damage in the United States (NOAA 2023) (table S1). The 72 h simulations before landfall reveal how the intensity and structure of hurricanes vary with the magnitude of spray-mediated sensible and latent heat fluxes. To better understand the response of hurricanes by these implemented heat fluxes, we compared the simulation results against *in-situ* dropsonde data.

2. Materials and methods

2.1. Spray-mediated sensible and latent heat fluxes

Following Andreas's previous research works, the total latent and sensible heat fluxes ($H_{L,T}$ and $H_{S,T}$) in a numerical model can be partitioned as

$$H_{L,T} = H_{L,\mathrm{int}} + \alpha Q_L \quad (1)$$

$$H_{S,T} = H_{S,\mathrm{int}} + \beta Q_S - (\alpha - \gamma) Q_L \quad (2)$$

where $H_{L,int}$ and $H_{S,int}$ are the conventional interfacial latent and sensible heat fluxes, and α, β, and γ are nondimensional and non-negative parameters. Spray latent and sensible heat fluxes (Q_L and Q_S) are defined as $S_a W \Lambda(h) B(T_a) \rho_a L_v [q_s(T_a) - q]$ and $S_v W \Lambda(h) \rho_w c_{pw} (T_s - T_a)$, respectively, as described by Fairall *et al* (1994). Theses formulations are suitable for wave-coupled simulations. Here, ρ_a is the air density, ρ_w is the seawater density, W is the whitecap fraction, L_ν is the latent heat of vaporization of water, c_{pw} is the specific heat of seawater, $B(T_a)$ and $\Lambda(h)$ are the correction factors, S_a is the moisture flux-related parameter of 0.125 s^{-1}, S_v is the relevant whitecap normalized droplet volume flux of 5.0×10^{-6} m s^{-1}, $T_s - T_a$ is the air-sea temperature difference, q_s is the saturation specific humidity, and q is the specific humidity.

In equations (1) and (2), non-negative parameters α, β, and γ control the proportion of the spray-related terms in the total heat fluxes. The term αQ_L represents the spray-mediated latent heat flux contributed by the evaporation of the spray droplets. Meanwhile, the term $\beta Q_S - (\alpha - \gamma) Q_L$ in equation (2) denotes the spray-mediated sensible heat flux, describing the collective energy transfer by the individual sea spray droplet from the ocean surface to the lower atmosphere. The term γQ_L is a correction factor for the increased near-surface temperature gradient caused by the evaporation of sea spray. Note that the αQ_L is subtracted from the $H_{S,T}$ to conserve energy due to evaporative cooling in equation (2).

2.2. Model descriptions

We utilize the COAWST modeling system (Warner *et al* 2010), composed of various community models interfaced through the model coupling toolkit (MCT). Our study employs Weather Research and Forecasting (WRF) (Skamarock *et al* 2019) for the atmospheric component, the Regional Ocean Model System (ROMS) (Haidvogel *et al* 2008, Shchepetkin and McWilliams 2009) for the ocean component, and the WAVEWATCH-III (hereafter WW3) (WAVEWATCH III Development Group 2016) for the wave component. These components exchange variables every 10 min via MCT, but our study excludes wave-current interactions between ROMS and WW3.

The WRF model consists of one outer and two nested inner domains with resolutions of 9, 3, and 1 km, respectively (figure S1). The nested inner domains are positioned along each hurricane trajectory (not shown). Physics schemes include the WSM 6-class Graupel scheme for microphysics (Hong and Lim 2006), the Korean Integrated Model Simplified Arakawa–Schubert scheme for cumulus (Kwon and Hong 2017), the New Simplified Arakawa–Schubert shallow cumulus scheme for shallow cumulus (Han and Pan 2011), and the Shin-Hong scale-aware scheme for the planetary boundary layer (PBL) (Shin and Hong 2013). The surface heat flux formulation follows the revised MM5 surface layer scheme (Jiménez *et al* 2012). The WRF is initialized on each specified date of initialization, 72 h before their landfall (e.g. 27 August 2021, for Hurricane Ida), using

the National Centers for Environmental Prediction Final analysis data (GDAS-FNL 2015) for initial and boundary conditions, updating lateral boundary conditions every 6 h.

ROMS has a single domain that matches WRF's outer domain, and it employs a double stretching function (Shchepetkin and McWilliams 2009) to define the 32 vertical levels. Specifically, ROMS utilizes a third-order upstream horizontal advection scheme, a fourth-order centered vertical advection scheme, and a generic large-scale vertical mixing scheme (Umlauf and Burchard 2003, Warner *et al* 2005). ROMS integrates tidal information from TPXO8-atlas (Egbert and Erofeeva 2002) at open boundaries, including eight tidal constituents: Q1, O1, P1, K1, N2, M2, S2, and K2. Initial and lateral boundary conditions are derived from the Hybrid Coordinate Ocean Model (HYCOM) (Cummings 2006) analysis data, and its bathymetry is based on the 1 min Gridded Global Relief Data.

WW3 shares the same spatial domain as ROMS, using 24 frequency and 25 direction bins for spectral resolution. It explicitly solves directional wave spectra, accounting for whitecap dissipation, nonlinear wave interactions, and wave breaking. Specifically, we have modified the coupling framework to allow the whitecap fraction from the whitecap dissipation package (Ardhuin *et al* 2010) in WW3 to be passed to WRF via MCT. The whitecap fraction is then utilized to calculate the spray latent and sensible heat fluxes (Q_L and Q_S).

The COAWST system without sea spray parameterization was carefully tuned to ensure its performance aligns with standard air–sea coupled modeling experiments (e.g. Bae *et al* 2022, Yang *et al* 2022). This system is a reliable baseline for incorporating the effects of spray-mediated heat fluxes, as described by Olabarrieta *et al* (2012).

2.3. Hurricane detection and tracking method

To determine the best positions and intensities at 6 h intervals throughout a hurricane's lifecycle, we use the National Hurricane Center (NHC)'s best track dataset from the Atlantic hurricane database (HURDAT2) (Landsea and Franklin 2013). HURDAT2 provides information such as the best locations, minimum sea-level pressure, and maximum surface wind speed. Since 2005, the National Oceanic and Atmospheric Administration (NOAA) has been advancing this field with annual hurricane field programs (Rogers *et al* 2006). We use vertical wind profiles from the dropsonde data near the hurricane center to assess hourly model results. To evaluate the hourly model errors, we first reduce noise by smoothing the profile with a 5 s lowpass filter (Powell *et al* 2003) and round the observed time to the nearest hour. We average the wind profiles across altitudes using 100 m bins up to 3 km height. This noise reduction and averaging greatly reduces variability on scales not captured by the model but cannot entirely remove it. By employing cubic splines, we interpolate positions and intensities from HURDAT2 to 1 h intervals for direct comparison with dropsonde data. Finally, we detect and track hurricanes from our simulations using the Geophysical Fluid Dynamics Laboratory vortex tracker (Biswas *et al* 2018). After the hurricane detection, we compute hourly hurricane-relative tangential and radial winds at all altitudes and locations in the dropsonde data. These computations are based on the best locations given by HURDAT2. Rapid intensification is defined as an increase in maximum sustained winds of at least 30 kt (15.4 m s^{-1}) within 24 h, following the criteria established by Kaplan and DeMaria (2003).

2.4. Model error estimation

In figures 1, 2 and S3 the model error for all simulations is determined by estimating the normalized root-mean-square error (NRMSE), a unitless measure of the prediction error in forecast performance against reliable observations. The NRMSE is defined as follows:

$$\mathrm{NRMSE} = \sqrt{\frac{\sum (x_{\mathrm{obs}} - x_{\mathrm{mod}})^2}{\sum (x_{\mathrm{obs}} - \overline{x_{\mathrm{obs}}})^2}}, \qquad (3)$$

where x_{obs} is the observed value, x_{mod} is the simulated value, and the overbar denotes the arithmetic mean. As noted in the main text, we compare the key prognostic variables, including minimum sea level pressure (P_{min}), maximum surface wind speed (V_{max}), and tangential and radial wind speeds (V_{tan} and V_{rad}) at 1 km above sea level. These variables are key parameters that represent hurricane intensity in the numerical hurricane model.

For P_{min} and V_{max}, the NRMSEs for all simulations are estimated using the observed time series at 6 h intervals from HURDAT2. In contrast, the NRMSEs for V_{tan} and V_{rad} at 100 m height intervals up to 3 km height are estimated using 126 wind profiles located within a 500 km radius of the hurricane center and corresponding to a 72 h forecast period. For example, figures 1(c) and (d) shows the NRMSE at 1 km height above the sea surface, while figure S3 shows the NRMSE profile vertically up to 3 km height. In particular, figure S2 provides rankings based on a unitless scoring metric by averaging the NRMSEs of all the variables shown in figure 1. The normalized mean error used to score the ranking of the sensitivity

experiments is defined as follows:

$$\overline{\mathrm{NRMSE}} = \frac{1}{4}\left[\mathrm{NRMSE}_{P_{\min}} + \mathrm{NRMSE}_{V_{\max}} + \mathrm{NRMSE}_{V_{\tan}} + \mathrm{NRMSE}_{V_{\mathrm{rad}}}\right], \quad (4)$$

where $\overline{\mathrm{NRMSE}}$ is the average of the NRMSE for the four prognostic key variables, $P_{\min}$, $V_{\max}$, $V_{\tan}$ and V_{rad}. These NRMSE values are derived as a function of α and β in the sensitivity experiments.

3. Results

3.1. Sensitivity to the key parameters

To examine how much hurricane intensity is sensitive to the magnitude of the two key parameters in equations (1) and (2), we performed 28 sensitivity tests for Hurricane Ida (2021), which intensified rapidly over the Gulf of Mexico from 27 August to 30 August 2021. Here, an array of four α values from 0 to 3.75 by 1.25 and seven β values from 0 to 15 by 2.5 are used for the sensitivity test. The γ value is set to be $\alpha - 0.5$ in all experiments, based on the range of their values suggested by previous papers (Andreas 2003, Andreas *et al* 2008, 2015). These key parameters directly control the proportion of the spray-mediated heat fluxes to the turbulent heat flux.

For a comprehensive assessment of forecast performance, we provide a heat map that displays the NRMSE by normalizing standard deviations (figure 1). The hurricane intensities are represented by the minimum sea-level pressure ($P_{\min}$), and maximum surface wind speed ($V_{\max}$), and tangential and radial velocities at 1 km height above the sea surface. Two separate observation data sets were used to compare with the model results: the HURDAT2 best track data and the GPS dropsonde data available for the Ida case at the Hurricane Research Division.

We find that, compared to the control simulation where α and β are 0 (i.e. no spray effect), increasing β dramatically reduces the error for hurricane intensity, while increasing the α value for a fixed β has no notable effect on reducing the error. In equation (2), α modifies the magnitude of evaporation from the sea spray and β controls the magnitude of the spray-mediated sensible heat flux. It can be interpreted that the model error for hurricane intensity decreases with an increase in the spray-mediated sensible heat flux but is less sensitive to variations in evaporations of sea spray. Each hurricane intensity variable has a different combination of α and β values for the minimum errors, but β values higher than 10 consistently show a better result for all four intensity variables.

To obtain a more comprehensive measure of the forecast performance, we calculate a unitless scoring metric by averaging the NRMSEs of all the four intensity variables shown in figure 1, highlighting the lowest error in the heat map with a red box. In figure S2, we provide the scores along with the average of the aggregated NRMSEs. We find that the highest score occurred at $\alpha = 2.5$ and $\beta = 10$, which is within the range proposed in previous studies (Andreas 2003, Andreas *et al* 2008, 2015) (see circle, triangle, and square in figure 1). Additionally, we compared the vertical profiles of simulated winds to dropsonde and found improved performance in the $\alpha = 2.5$ and $\beta = 10$ simulation (figure S3). The radial velocity error was reduced from the surface to 1.5 km altitude, and the tangential velocity error was reduced above 500 m altitude.

3.2. Spray-mediated hurricane intensification

The simulated azimuthal mean structure is analyzed along the radial distance for Hurricane Ida with a simulation by setting $\alpha = 2.5$ and $\beta = 10$, which we call SPRAY. We also refer to a coupled simulation without sea spray ($\alpha = 0$ and $\beta = 0$) as CPL and an uncoupled simulation with only the WRF as UNCPL. Here we focus on the temporal and azimuthal averages during the 36–60 simulation hour, which represents intensification phase over the Gulf of Mexico (see figure 3 for intensity time series).

Figure 2 provides the characteristics of radial wind in SPRAY, which exhibits intense lower-level frictional inflow near the PBL and distinct upper-level outflow. This process results in enhancing the secondary circulation (Emanuel 1986, Rousseau-Rizzi and Emanuel 2019). It is noteworthy that CPL and UNCPL exhibit relatively weaker radial inflow and outflow when compared to SPRAY. With the enhanced secondary circulation, the increased radar reflectivity in SPRAY is a consequence of the slantwise deeper convection with stronger upward motions around the radius of maximum tangential wind speed (RMW). Notably, the distribution pattern of the radar reflectivity aligns closely with that of the tangential wind. Furthermore, within the region of the RMW, SPRAY exhibits a distinct and strong vortex warm core in terms of temperature deviations. This feature is characterized by a stronger radial temperature gradient compared to UNCPL and CPL.

As the sea spray evaporates, it physically induces changes in low-level atmospheric cooling and moisture and temperature gradients near the surface. Simultaneously, spray-mediated sensible heat exchanges occur, leading to a substantial increase in the total sensible heat flux ($H_{S,T}$), which is comparable in magnitude to the total latent heat flux ($H_{L,T}$). This increased upward $H_{S,T}$ warms the near-surface atmosphere, subsequently reducing the temperature gradient and relative humidity. A comparative analysis of CPL and SPRAY focusing on the interfacial, spray-mediated, and total heat fluxes is presented in figure S4. In SPRAY, a whitecap of up to ~5% is formed around the hurricane center (figure S5(a)). Consequently, the interfacial sensible heat flux ($H_{S,\mathrm{int}}$) in SPRAY exhibits a smaller value compared to that in CPL, while the interfacial latent heat flux

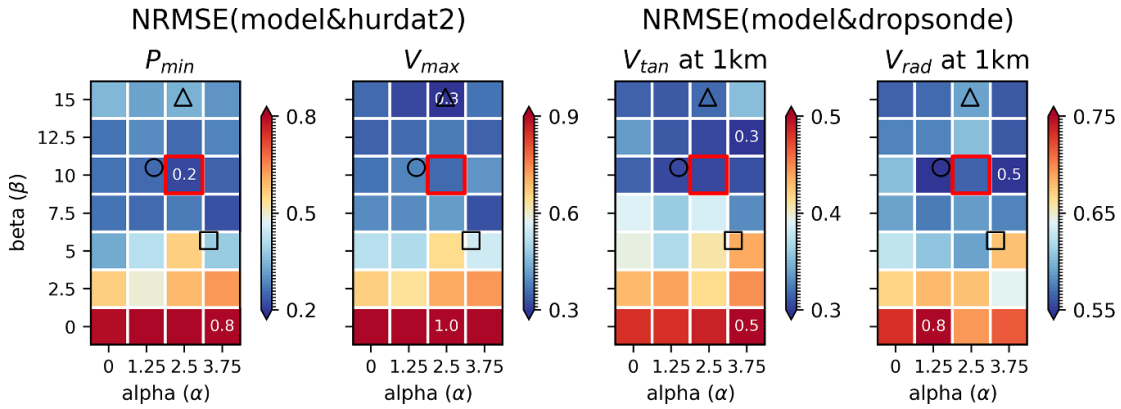

Figure 1. Heat map of the normalized root-mean-squared errors (NRMSEs) by normalizing the observed standard deviation for the minimum sea-level pressure ($\boldsymbol{P}_{\mathbf{min}}$), maximum surface wind speed ($\boldsymbol{V}_{\mathbf{max}}$), and tangential and radial velocities ($\boldsymbol{V}_{\mathbf{tan}}$ and $\boldsymbol{V}_{\mathbf{rad}}$) at 1 km above the sea surface of 28 sensitivity experiments, varying four $\boldsymbol{\alpha}$ values from 0 to 3.75 by 1.25 and seven $\boldsymbol{\beta}$ values from 0 to 15 by 2.5. Each panel shows the minimum and maximum values in white. The red box denotes the lowest average value of the aggregated NRMSE for all the four intensity variables (see equation (4)). The color scheme represents unitless NRMSE scores to emphasize different sets of two key parameters. The circle, square, and triangle symbols indicate the location of sets proposed by Andreas's research works (Andreas 2003, Andreas *et al* 2008, 2015), respectively. The NRMSEs for $\boldsymbol{P}_{\mathbf{min}}$ and $\boldsymbol{V}_{\mathbf{max}}$ are computed based on the HURDAT2 best track data ($n = 12$), whereas the NRMSEs for $\boldsymbol{V}_{\mathbf{tan}}$ and $\boldsymbol{V}_{\mathbf{rad}}$ at 1 km are computed based on the GPS dropsonde observations available ($n = 126$). More details on how to estimate model error can be found in the materials and methods section.

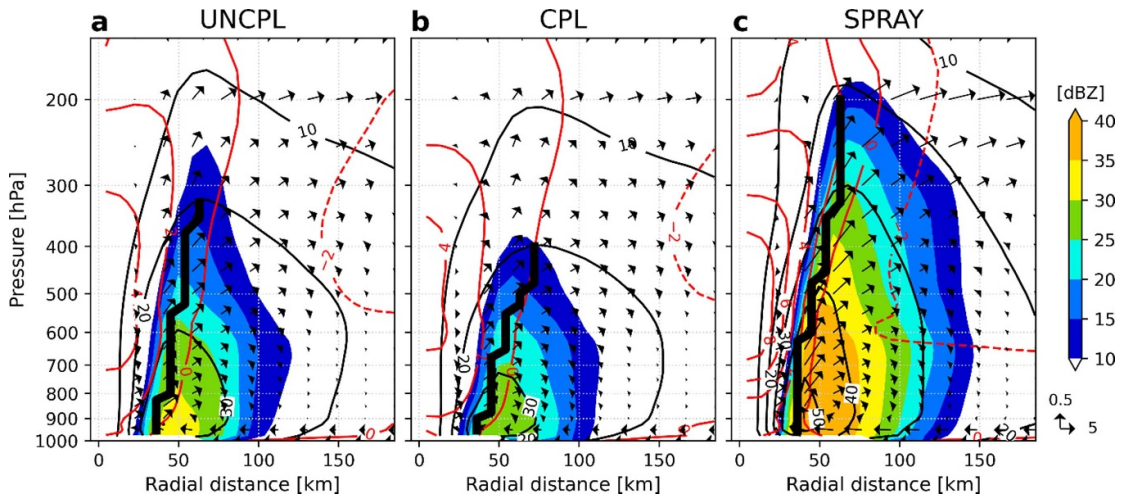

Figure 2. Radius–pressure cross-sections of azimuthally and temporally (from the 36 h to 60 h) averaged radar reflectivity [dBZ] (color shadings), radial and vertical wind components (m s^{-1}) (black arrows), potential temperature deviation [K] (red contour), and tangential wind speed (m s^{-1}) (black contour) for (a) UNCPL, (b) CPL, and (c) SPRAY simulations. The thick black line denotes the radius (km) of maximum tangential wind (RMW) > 20 m s^{-1}. The potential temperature deviation is defined at each vertical level as the deviation from the mean for a horizontal area within a radius of 180 km.

($H_{L,\mathrm{int}}$) in SPRAY demonstrates a larger value compared to that in CPL. The presence of spray-mediated heat fluxes significantly amplifies the sum of the $H_{S,T}$ and $H_{L,T}$ (referred to as turbulent heat flux), which are recognized as an essential driver of energy for hurricanes (Businger 1982, Emanuel 1995, Zhang *et al* 2008).

The turbulent kinetic energy (TKE), an important metric of turbulence mixing, is related to the transport of momentum, heat, and moisture, as well as the kinetic energy dissipation rate in the boundary layer (Stull 1988). In particular, the strong sensible heating under the PBL increases the near-surface TKE in SPRAY (figure S5(d)). Therefore, given strong near-surface heating, buoyant eddies mix efficiently to the top of the boundary layer, transferring heat upward against the mean potential temperature gradient (Kepert 2012). It is noteworthy that the presence of sea spray further enhances this process, thereby amplifying the overall intensity of the hurricane. Of particular note is that sea spray leads to a significant enhancement of the sensible heat flux ($H_{S,T}$), especially when compared to the latent heat flux ($H_{L,T}$).

3.3. Recent rapid intensification cases

To further test whether the presence of spray-mediated heat fluxes is an important factor in

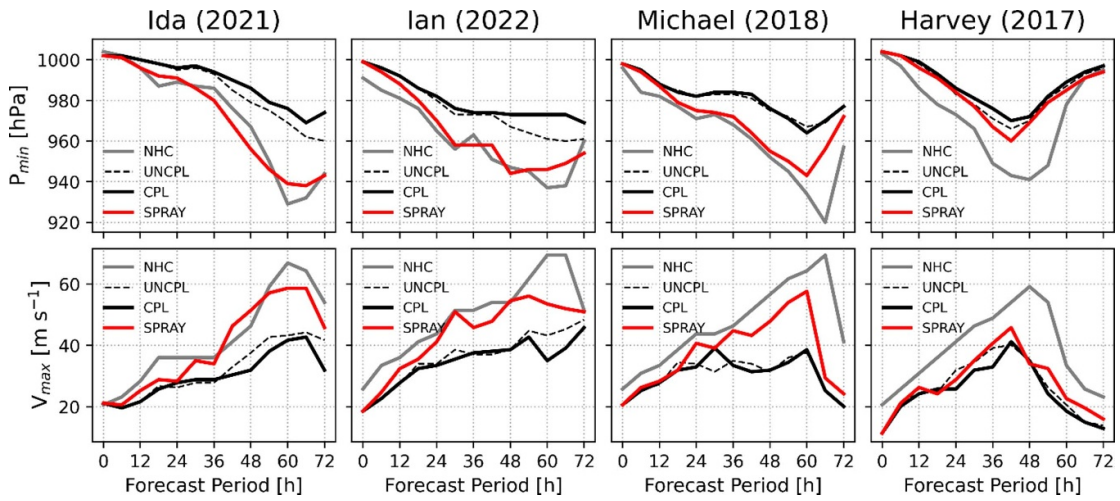

Figure 3. Time series of (top) center pressure $\boldsymbol{P_{min}}$ (hPa) and (bottom) maximum wind speed $\boldsymbol{V_{max}}$ (m s^{-1}) for the UNCPL, CPL, and SPRAY simulations and the best track data from NHC during Hurricanes Ida (2021), Ian (2022), Michael (2018), and Harvey (2017).

improving hurricane intensity forecasts of P_{min} and V_{max}, we performed additional simulations of Hurricanes Harvey, Michael, and Ian, whose summary statistics are listed in table S1. All simulated tracks are similar to the observed track from the NHC (figure S6). The presence or absence of sea spray does not affect the accuracy of the hurricane track forecasts for our cases.

Unlike the simulated tracks, there are significant differences in the simulated intensity, both P_{min} and V_{max} for all hurricane cases, though less markedly so for Harvey. Figure 3 compares the time series of P_{min} and V_{max} at 6 h intervals for UNCPL, CPL, and SPRAY simulations and the NHC observed data for the forecast period of 72 h after each initialization. It is evident that the SPRAY substantially improves the hurricane intensity forecast, capturing the observed rapid intensification of the hurricanes compared to the CPL and UNCPL simulations. For Ida, SPRAY shows that P_{min} drops to 942 hPa and V_{max} increases to $\sim$60 m s^{-1}.

The overall temporal evolution of P_{min} and V_{max} in SPRAY is significantly improved in comparison with the NHC best track intensity, whereas UNCPL and CPL do not capture rapid intensification. The CPL intensities are even weaker than the UNCPL intensities. This result demonstrates that ocean coupling in the model could suppress hurricane intensity through air-sea interaction in some cases. Intense hurricane can cause ocean upwelling, and cooler sea surface temperatures are not conductive to rapid intensification (Emanuel 1999, Schade and Emanuel 1999). It is inferred that this negative feedback from sea surface cooling could be diminished in CPL simulations without incorporating sea spray processes. Despite the initialization biases in vortex intensity, as noted by V_{max} differences between SPRAY and NHC at 0 h for Ian, Michael, and Harvey in figure 3, it is remarkable that SPRAY could reproduce the observed rapid intensification. The larger errors in Harvey case from SPRAY could be attributed to its relatively weaker initial intensity, which induces less spray impact. Harvey's initial maximum wind speed in the simulations was $\sim$10 m s^{-1}, unlike other hurricanes with higher initial wind speeds $>$ 20 m s^{-1}.

4. Discussion and conclusions

This study investigated the impact of spray-mediated heat fluxes on hurricane intensification events using the COAWST modeling system. The results demonstrated that incorporating the sea spray into the system improves the prediction of hurricane intensity, especially for rapid intensification cases. Specifically, we found optimal ranges of α and β parameters for the existing spray flux parameterization through a comprehensive sensitivity test. These parameters directly control the proportion of the spray-mediated heat fluxes to the turbulent heat flux.

The sensitivity test revealed that increasing β leads to a substantial reduction in errors for key prognostic variables associated with hurricane intensity against best track data and *in-situ* dropsonde data. On the other hand, variations in α have less impact on the errors. These results underscore that the sensible heat flux, rather than latent heat flux, is likely the main route by which spray affects hurricane energetics. These findings follow the work of Andreas and extend recent studies by Xu *et al* (2023).

To better illustrate the hurricane intensification mechanism incorporating the sea spray processes, we provide a schematic illustration in figure 4. Additionally, we explored the physical mechanisms that intensify the hurricane in this study. Based on

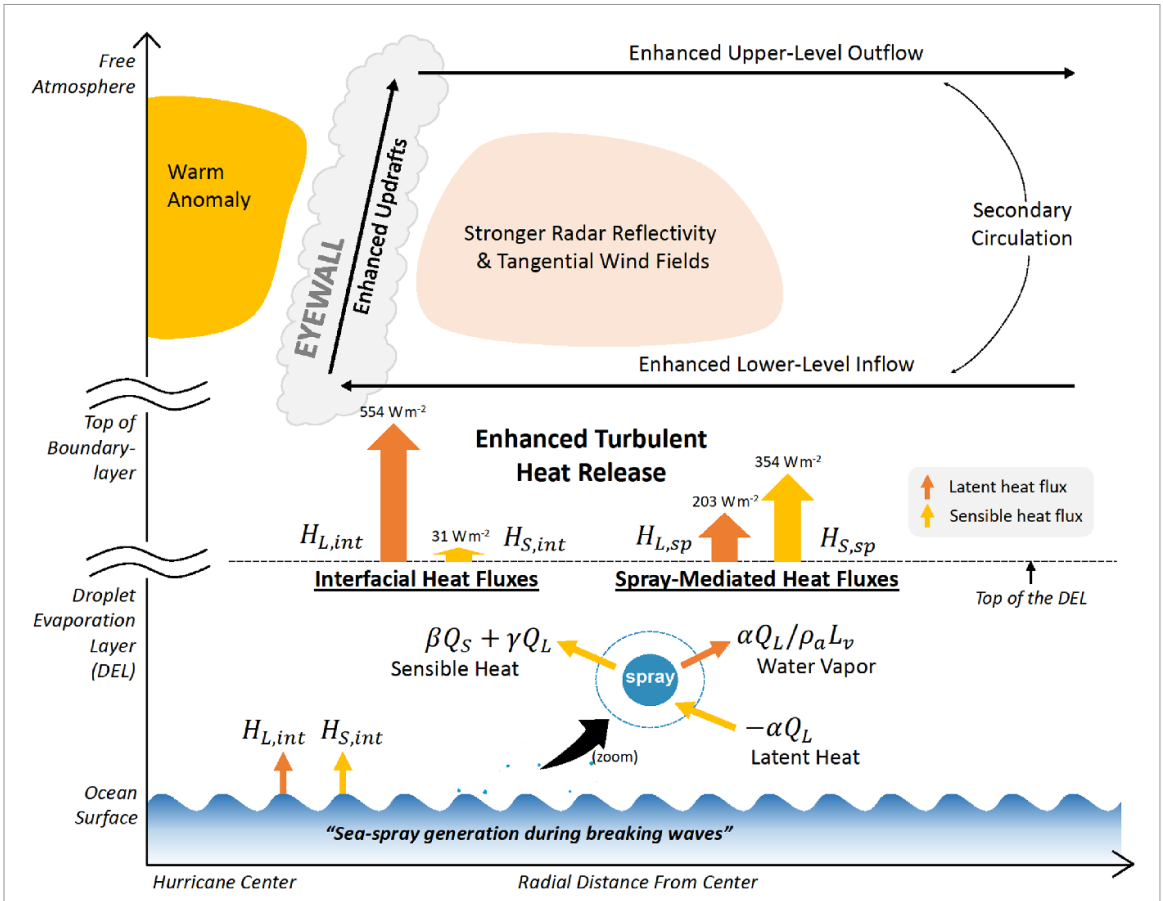

Figure 4. Schematic illustration of proposed mechanisms for intensifying hurricanes in this study. All properties were set up based on figures 2, S4 and S5. The sea spray processes in the droplet evaporation layer (DEL) were represented according to the description of AN15. The values above each heat flux symbol at the top of the DEL were the radial and azimuthal mean heat fluxes during the 36–60 h intensification phase of Hurricane Ida.

the comparison shown in figure 2, SPRAY exhibits distinct characteristics in the radial structure of hurricanes. The presence of sea spray within the droplet evaporation layer results in enhanced turbulent heat release (figure S5), lower-level inflow, upper-level outflow, and deeper convection (figure 2), leading to stronger winds and vortex warm cores near the hurricane center. These findings indicate the importance of sea spray in modulating the secondary circulation and convective activity of hurricanes consistent with recent studies (Wada *et al* 2018).

The high spatial and temporal resolution of dropsonde observations enable a precise comparison between modeled and observed hurricane structures. By using dropsonde data, our extensive sensitivity tests reveal a new set of two key parameters ($\alpha = 2.5$ and $\beta = 10$) for spray flux parameterization. These parameters are centered on the suggestions of Andreas (different markers in figure 1). This approach highlights the value of dropsonde data in understanding uncertainty in the flux parameterization used for hurricane simulations. It is more common to compare model simulations against best-track intensity only. However, *in-situ* dropsonde data allowed us to examine the impact of model results on the local vertical wind profiles. Although direct flux observations under hurricanes are scarce, near-surface dropsonde observations provide valuable avenues to verify the accuracy of flux parameterizations. We believe that integrating more *in-situ* near-surface observations in model verifications and sensitivity tests could significantly enhance our understanding of air–sea interactions.

While these parameters ($\alpha = 2.5$ and $\beta = 10$) improve accuracy in our cases, it is important to note that they were derived from dropsonde data for a specific hurricane. To validate the robustness of our findings, we extended our analysis beyond Hurricane Ida to include additional three hurricanes (Ian, Michael, and Harvey) and four typhoons (Maysak, Bavi, Lingling, and Soulik), as presented in table S2. Although typhoon experiments are preliminary results, this supplementary table demonstrates the applicability of our approach to various tropical cyclone cases and summarize the intensity errors. In all cases, the SPRAY simulations consistently showed lower RMSE compared to the CPL simulations. The reduction rate in RMSE for $P_{\min}$ ranged from 9.1% to 74.4%, indicating a consistent improvement in intensity prediction.

In conclusion, this study strengthens insights into the distinguished role of sea spray in turbulent heat exchange that drives hurricane rapid intensification raised by previous studies. By highlighting the differential impacts of spray-mediated sensible and latent heat fluxes and identifying key parameters for improved simulations, we contribute to the ongoing efforts to enhance hurricane intensity predictions.

Future research should focus on expanding the number of case studies, obtaining direct sea spray measurements, testing these findings across a wider range of hurricane intensities and environmental conditions, examining potential variations in different ocean basins or climate regimes, and assessing sensitivity to model resolution and physics schemes. For example, the WRF physical parameterizations used in this study may be specific to our research. Previous studies (e.g. Li and Pu 2008, Torn and Davis 2012) have shown that different combinations of physical parameterizations can impact WRF model simulation results. Therefore, sensitivity experiments on various physical schemes, particularly those incorporating sea spray effects, will be crucial for model optimization and improving hurricane predictions.

Data availability statement

The GPS dropsonde data can be accessed at the NOAA Hurricane Research Division website (www.aoml.noaa.gov/data-products/#hurricanedata). In addition, the NOAA National Hurricane Center (NHC) provides the best track data from its Atlantic hurricane database (HURDAT2) at www.nhc.noaa.gov/data/hurdat/hurdat2-1851-2022-050423.txt. Data for the coupled model are available online from the NCEP GDAS/FNL (https://doi.org/10.5065/D65Q4T4Z) and HYCOM analysis (www.hycom.org/dataserver/gofs-3pt1/analysis).

The data that support the findings of this study are openly available at the following URL/DOI: https://figshare.com/s/931c46543c04a593629d.

Acknowledgment

This work was funded by research grants funded by the Korea Hydrographic and Oceanographic Agency (KHOA), the Ministry of Oceans and Fisheries (MOF), Korea. This work was supported by Korea Environment Industry & Technology Institute (KEITI) through "Climate Change R&D Project for New Climate Regime", funded by Korea Ministry of Environment (MOE) (RS-2022-KE002160). This work was also supported by the National Research Foundation of Korea (NRF) grant funded by the Korea government (MSIT) (No. NRF-2022R1A2C1006788). S Y was supported by the Korea Meteorological Administraation Research and Development Program "APEC Climate Center for Climate Information Services" under Grant (KMA2013-07510). We would also thank H-J Bae for his valued assistance in conducting our hurricane simulations and G Kim for helping to create the schematics shown in figure 4.

ORCID iDs

Sinil Yang https://orcid.org/0000-0002-8851-6495
Mark Bourassa https://orcid.org/0000-0003-3345-9531
Dong-Hyun Cha https://orcid.org/0000-0001-5053-6741
Baek-Min Kim https://orcid.org/0000-0002-1717-183X

References

Andreas E L 1992 Sea spray and the turbulent air-sea heat fluxes *J. Geophys. Res.* **97** 429–41
Andreas E L 2003 An algorithm to predict the turbulent air-sea fluxes in high-wind, spray conditions *Environ. Sci.* 7 (available at: http://ams.confex.com/ams/pdfpapers/52221.pdf)
Andreas E L and Decosmo J 2002 The signature of sea spray in the hexos turbulent heat flux data *Bound.-Layer Meteorol.* **103** 303–33
Andreas E L and Emanuel K A 2001 Effects of sea spray on tropical cyclone intensity *J. Atmos. Sci.* **58** 3741–51
Andreas E L, Mahrt L and Vickers D 2015 An improved bulk air-sea surface flux algorithm, including spray-mediated transfer *Q. J. R. Meteorol. Soc.* **141** 642–54
Andreas E L and Monahan E C 2000 The role of whitecap bubbles in air-sea heat and moisture exchange *J. Phys. Oceanogr.* **30** 433–42
Andreas E L, Persson P O G and Hare J E 2008 A bulk turbulent air-sea flux algorithm for high-wind, spray conditions *J. Phys. Oceanogr.* **38** 1581–96
Ardhuin F *et al* 2010 Semiempirical dissipation source functions for ocean waves. Part I: definition, calibration, and validation *J. Phys. Oceanogr.* **40** 1917–41
Bae H J, Yang S, Jeong T B, Yang A R, Cha D H, Lee G, Lee H Y, Byun D S and Kim B M 2022 An estimation of ocean surface heat fluxes during the passage of typhoon at the ieodo ocean research station: typhoon lingling case study 2019 *Asia-Pacific J. Atmos. Sci.* **58** 305–14
Bao J W, Fairall C W, Michelson S A and Bianco L 2011 Parameterizations of sea-spray impact on the air-sea momentum and heat fluxes *Mon. Weather Rev.* **139** 3781–97
Bianco L, Bao J W, Fairall C W and Michelson S A 2011 Impact of sea-spray on the atmospheric surface layer *Bound.-Layer Meteorol.* **140** 361–81
Biswas M K, Stark D and Carson L 2018 GFDL vortex tracker users guide version 3.9a (National Center for Atmospheric Research and Developmental Testbed Center)
Black P G, D'Asaro E A, Drennan W M, French J R, Niiler P P, Sanford T B, Terrill E J, Walsh E J and Zhang J A 2007 Air-sea exchange in hurricanes *Bull. Am. Meteorol. Soc.* **88** 357–74
Businger J A 1982 The fluxes of specific enthalpy, sensible heat and latent heat near the earth's surface *J. Atmos. Sci.* **39** 1889–92
Cummings J A 2006 Operational multivariate ocean data assimilation *Q. J. R. Meteorol. Soc.* **131** 3583–604
Egbert G D and Erofeeva S Y 2002 Efficient inverse modeling of barotropic ocean tides *J. Atmos. Ocean. Technol.* **19** 183–204
Emanuel K A 1986 An air-sea interaction theory for tropical cyclones. Part I: steady-state maintenance *J. Atmos. Sci.* **43** 585–604

Emanuel K A 1995 Sensitivity of tropical cyclones to surface exchange coefficients and a revised steady-state model incorporating eye dynamics *J. Atmos. Sci.* **52** 3969–76
Emanuel K A 1999 Thermodynamic control of hurricane intensity *Nature* **401** 665–9
Emanuel K A, Velez-pardo M and Cronin T W 2023 The surprising roles of turbulence in tropical cyclone physics pp 1–14
Fairall C W, Banner M L, Peirson W L, Asher W and Morison R P 2009 Investigation of the physical scaling of sea spray spume droplet production *J. Geophys. Res.* **114** 1–19
Fairall C W, Kepert J D and Holland G J 1994 The effect of sea spray on surface energy transports over the ocean *Glob. Atmos. Ocean Syst.* **2** 121–42
GDAS-FNL 2015 NCEP GDAS/FNL 0.25 degree global tropospheric analyses and forecast grids (National Centers for Environmental Prediction, National Weather Service, NOAA, U.S. Department of Commerce) 10.5065/D65Q4T4Z
Haidvogel D B *et al* 2008 Ocean forecasting in terrain-following coordinates: formulation and skill assessment of the regional ocean modeling system *J. Comput. Phys.* **227** 3595–624
Han J and L P H 2011 Revision of convection and vertical diffusion schemes in the NCEP global forecast system *Weather Forecast.* **26** 520–33
Holthuijsen L H, Powell M D and Pietrzak J D 2012 Wind and waves in extreme hurricanes *J. Geophys. Res. Ocean.* **117** 1–15
Hong S-Y and Lim J-O 2006 The WRF single-moment 6-class microphysics scheme (WSM6) *Asia-Pacific J. Atmos. Sci.* **42** 129–51
Jiménez P A, Dudhia J, González-Rouco J F, Navarro J, Montávez J P and García-Bustamante E 2012 A revised scheme for the WRF surface layer formulation *Mon. Weather Rev.* **140** 898–918
Kaplan J and DeMaria M 2003 Large-scale characteristics of rapidly intensifying tropical cyclones in the North Atlantic basin *Weather Forecast.* **18** 1093–108
Kepert J D 2012 Choosing a boundary layer parameterization for tropical cyclone modeling *Mon. Weather Rev.* **140** 1427–45
Kwon Y C and Hong S Y 2017 A mass-flux cumulus parameterization scheme across gray-zone resolutions *Mon. Weather Rev.* **145** 583–98
Lan Y, Leng H, Sun D, Song J and Cao X 2022 An improved sea spray-induced heat flux algorithm and its application in the case study of typhoon mangkhut (2018) *J. Mar. Sci. Eng.* **10** 1329
Landsea C W and Franklin J L 2013 Atlantic hurricane database uncertainty and presentation of a new database format *Mon. Weather Rev.* **141** 3576–92
Li X and Pu Z 2008 Sensitivity of numerical simulation of early rapid intensification of Hurricane Emily (2005) to cloud microphysical and planetary boundary layer parameterizations *Mon. Weather Rev.* **136** 4819–38
Liu B, Liu H, Xie L, Guan C and Zhao D 2011 A coupled atmosphere-wave-ocean modeling system: simulation of the intensity of an idealized tropical cyclone *Mon. Weather Rev.* **139** 132–52
NOAA 2023 Billion-dollar weather and climate disasters (National Centers for Environmental Information (NCEI) U.S.) (available at: www.ncei.noaa.gov/access/billions/)
Olabarrieta M, Warner J C, Armstrong B, Zambon J B and He R 2012 Ocean-atmosphere dynamics during Hurricane Ida and Nor'Ida: an application of the coupled ocean-atmosphere-wave-sediment transport (COAWST) modeling system *Ocean Modell.* **43–44** 112–37
Powell M D, Vickery P J and Reinhold T A 2003 Reduced drag coefficient for high wind speeds in tropical cyclones *Nature* **422** 279–83
Rogers R *et al* 2006 The intensity forecasting experiment: a NOAA multiyear field program for improving tropical cyclone intensity forecasts *Bull. Am. Meteorol. Soc.* **87** 1523–37
Rogers R *et al* 2013 NOAA'S hurricane intensity forecasting experiment: a progress report *Bull. Am. Meteorol. Soc.* **94** 859–82
Rousseau-Rizzi R and Emanuel K A 2019 An evaluation of hurricane superintensity in axisymmetric numerical models *J. Atmos. Sci.* **76** 1697–708
Schade L R and Emanuel K A 1999 The ocean's effect on the intensity of tropical cyclones: results from a simple coupled atmosphere-ocean model *J. Atmos. Sci.* **56** 642–51
Shchepetkin A F and McWilliams J C 2009 Correction and commentary for "Ocean forecasting in terrain-following coordinates: formulation and skill assessment of the regional ocean modeling system" by Haidvogel *et al*, J. Comp. Phys. 227, pp. 3595–3624 *J. Comput. Phys* **228** 8985–9000
Shin H H and Hong S Y 2013 Analysis of resolved and parameterized vertical transports in convective boundary layers at gray-zone resolutions *J. Atmos. Sci.* **70** 3248–61
Skamarock W C, Klemp J B, Dudhia J B, Gill D O, Barker D M, Duda M G, Huang X-Y, Wang W and Powers J G 2019 A description of the advanced research WRF version 4
Sroka S and Emanuel K A 2022 Sensitivity of sea-surface enthalpy and momentum fluxes to sea spray microphysics *J. Geophys. Res. Ocean.* **127** e2021JC017774
Staniec A, Vlahos P and Monahan E C 2021 The role of sea spray in atmosphere–ocean gas exchange *Nat. Geosci.* **14** 593–8
Stull R B 1988 *An Introduction to Boundary Layer Meteorology* (Springer Netherlands) (available at: https://books.google.co.kr/books?id=eRRz9RNvNOkC)
Torn R D and Davis C A 2012 The inuence of shallow convection on tropical cyclone track forecasts *Mon. Weather Rev.* **140** 2188–97
Umlauf L and Burchard H 2003 A generic length-scale equation for geophysical turbulence models *J. Mar. Res.* **61** 235–65
Wada A, Kanada S and Yamada H 2018 Effect of air-sea environmental conditions and interfacial processes on extremely intense Typhoon Haiyan (2013) *J. Geophys. Res. Atmos.* **123** 10379–405
Warner J C, Armstrong B, He R and Zambon J B 2010 Development of a coupled ocean-atmosphere-wave-sediment transport (COAWST) modeling system *Ocean Modell.* **35** 230–44
Warner J C, Sherwood C R, Arango H G and Signell R P 2005 Performance of four turbulence closure models implemented using a generic length scale method *Ocean Modell.* **8** 81–113
WAVEWATCH III Development Group 2016 User manual and system documentation of WAVEWATCH III version 5.16 *NOAA/NWS/NCEP/MMAB Tech. note* pp 1–326
Xu X, Voermans J J, Moon I J, Liu Q, Guan C and Babanin A V 2022 Sea spray impacts on tropical cyclone Olwyn using a coupled atmosphere-ocean-wave model *J. Geophys. Res. Ocean.* **127** 1–13
Xu X, Voermans J J, Zhang W, Zhao B, Qiao F, Liu Q, Moon I J, Janekovic I, Waseda T and Babanin A V 2023 Tropical cyclone modeling with the inclusion of wave-coupled processes: sea spray and wave turbulence *Geophys. Res. Lett.* **50** e2023GL106536
Yang S, Moon I J, Bae H J, Kim B M, Byun D S and Lee H Y 2022 Intense atmospheric frontogenesis by air–sea coupling processes during the passage of Typhoon Lingling captured at Ieodo Ocean Research Station *Sci. Rep.* **12** 1–14
Zhang J A, Black P G, French J R and Drennan W M 2008 First direct measurements of enthalpy flux in the hurricane boundary layer: the CBLAST results *Geophys. Res. Lett.* **35** 2–5